fully polymerized (see Table 2), although with a somewhat lesser control (the reactions were not optimized). Vinyl acetate, a substrate known to be reluctant to undergo ATRP, is not polymerized under the same reaction conditions.

Table 2. [$RuCl_2$(*p*-cymene)(PCy_3)]-catalyzed polymerization of various vinyl monomers.[a]

Monomer	Yield [%]	M_n[b]	M_w/M_n	f[c]
methyl methacrylate	100	41500	1.12	0.95
tert-butyl methacrylate	80	33500	1.2	0.95
isobornyl methacrylate	70	25000	1.2	1.1[d]
n-butyl acrylate	80	37500	1.95	0.85
styrene	64	28500	1.3	0.9
vinyl acetate	0	–	–	–

[a] Reaction conditions same as in Table 1, except for styrene (initiator, (1-bromoethyl)benzene; temperature, 110 °C). [b] Apparent M_n for poly(*tert*-butyl methacrylate), poly(isobornyl methacrylate), and poly(*n*-butyl acrylate) determined with PMMA calibration. For poly(methyl methacrylate) and polystyrene, PMMA and PS calibrations were used, respectively. [c] Initiation efficiency $f = M_{n,theor.}/M_{n,exp.}$ with $M_{n,theor.} = ([MMA]_0/[initiator]_0) \times M_w(MMA) \times$ conversion. [d] An initiation efficiency higher than 1 could mean that the PMMA calibration is not suitable for poly(isobornyl methacrylate).

However, similar reactions with methacrylic acid (MA) and 2-hydroxyethyl methacrylate (HEMA) are successful, as well as controlled copolymerizations (95% MMA/5% MA and 90% MMA/10% HEMA) ($M_w/M_n = 1.24$ and 1.17). Since ATRP requires a suitable adjustment between the structure of the monomer, initiator, and atom (or group of atoms) to provide reversible termination, the catalyst has to be fine-tuned to each monomer. This has been exemplified for *n*-butyl acrylate. For this monomer, the molecular weight distribution dropped from 1.9 to 1.4 simply by the use of P*i*Pr_3 as the phosphane (instead of PCy_3), which demonstrates the versatility of the catalyst system.

Experimental Section

All reagents and solvents were dried, distilled, and stored under nitrogen at −20 °C with conventional methods. Ruthenium complexes were synthesized and purified according to the literature.[9, 13, 14] Grubbs catalyst, [$RuCl_2$(=CHPh)(PCy_3)$_2$], was used as received (Strem).

Polymerization of MMA: Ruthenium complex (0.0116 mmol) was placed in a glass tube containing a bar magnet and capped by a three-way stopcock. The reactor was purged of air (three vacuum–nitrogen cycles) before methyl methacrylate (1 mL, 9.35 mmol), and the initiator (ethyl 2-bromo-2-methylpropionate 0.1 M in toluene, 0.232 mL) were added. All liquids were handled with dried syringes under nitrogen. The mixture was heated in a thermostated oil bath for 16 h at 85 °C and, after cooling, dissolved in THF and the product precipitated in heptane. The polymer was filtered off and dried overnight at 80 °C under vacuum.

Received: July 20, 1998 [Z12167IE]
German version: *Angew. Chem.* **1999**, *111*, 559–562

Keywords: P ligands · polymerizations · radical reactions · ruthenium

[1] C. J. Hawker, *Acc. Chem. Res.* **1997**, *30*, 373–382, and references therein.
[2] a) J. Xia, K. Matyjaszewski, *Macromolecules* **1997**, *30*, 7697–7700; b) K. Matyjaszewski, J.-L. Wang, T. Grimaud, D. A. Shipp, *Macromolecules* **1998**, *31*, 1527–1534; c) K. Matyjaszewski, Y. Nakagawa, C. B. Jasieczek, *Macromolecules* **1998**, *31*, 1535–1541; d) V. Percec, B. Barboiu, H.-J. Kim, *J. Am. Chem. Soc.* **1998**, *120*, 305–316; e) D. M. Haddleton, A. M. Heming, D. Kukulj, D. J. Duncalf, A. J. Shooter, *Macromolecules* **1998**, *31*, 2016–2018, and references therein.
[3] a) T. Ando, M. Kamigaito, M. Sawamoto, *Macromolecules* **1997**, *30*, 4507–4510; b) K. Matyjaszewski, M. Wei, J. Xia, N. E. McDermott, *Macromolecules* **1997**, *30*, 8161–8164.
[4] a) C. Granel, P. Dubois, R. Jérôme, P. Teyssié, *Macromolecules* **1996**, *29*, 8576–8582; b) H. Uegaki, Y. Kotani, M. Kamigaito, M. Sawamoto, *Macromolecules* **1997**, *30*, 2249–2253.
[5] P. Lecomte, I. Drapier, P. Dubois, P. Teyssié, R. Jérôme, *Macromolecules* **1997**, *30*, 7631–7633.
[6] G. Moineau, C. Granel, P. Dubois, R. Jérôme, P. Teyssié, *Macromolecules* **1998**, *31*, 542–544.
[7] a) T. Ando, M. Kamigaito, M. Sawamoto, *Tetrahedron* **1997**, *53*, 15445–15457; b) J. Ueda, M. Matsuyama, M. Kamigaito, M. Sawamoto, *Macromolecules* **1998**, *31*, 557–562.
[8] G. Moineau, P. Dubois, R. Jérôme, T. Senninger, P. Teyssié, *Macromolecules* **1998**, *31*, 545–547.
[9] A. Demonceau, A. W. Stumpf, E. Saive, A. F. Noels, *Macromolecules* **1997**, *30*, 3127–3136.
[10] A. Hafner, A. Mühlebach, P. A. van der Schaaf, *Angew. Chem.* **1997**, *109*, 2213–2216; *Angew. Chem. Int. Ed. Engl.* **1997**, *36*, 2121–2124.
[11] a) R. H. Grubbs, S. J. Miller, G. C. Fu, *Acc. Chem. Res.* **1995**, *28*, 446–452; b) M. Schuster, S. Blechert, *Angew. Chem.* **1997**, *109*, 2124–2145; *Angew. Chem. Int. Ed. Engl.* **1997**, *36*, 2036–2056; c) S. K. Armstrong, *J. Chem. Soc. Perkin Trans. 1* **1998**, 371–388; d) R. H. Grubbs, S. Chang, *Tetrahedron* **1998**, *54*, 4413–4450, and references therein.
[12] a) W. A. Herrmann, M. Elison, J. Fischer, C. Köcher, G. R. J. Artus, *Chem. Eur. J.* **1996**, *2*, 772–780; b) W. A. Herrmann, C. Köcher, L. J. Gooßen, G. R. J. Artus, *Chem. Eur. J.* **1996**, *2*, 1627–1636.
[13] R. A. Zelonka, M. C. Baird, *Can. J. Chem.* **1972**, *50*, 3063–3072.
[14] M. A. Bennett, A. K. Smith, *J. Chem. Soc. Dalton Trans.* **1974**, 233–241.
[15] Y. Kotani, M. Kato, M. Kamigaito, M. Sawamoto, *Macromolecules* **1996**, *29*, 6979–6982.
[16] C. A. Tolman, *Chem. Rev.* **1977**, *77*, 313–348.

Modeling the Selectivity of Potassium Channels with Synthetic, Ligand-Assembled π Slides**

Maureen M. Tedesco, Bereket Ghebremariam, Naomi Sakai, and Stefan Matile*

Since Hodgkin and Huxley's demonstration almost fifty years ago that nerve signals originate from selective flux of Na^+ and K^+ ions across cell membranes, the mechanism of ion selectivity, particularly that of K^+ channels, has remained a fascinating and central question in life sciences.[1–3] The classical view of amide oxygen atoms serving as selective K^+ binding sites has received substantial support from site-

[*] Prof. S. Matile, M. M. Tedesco, B. Ghebremariam, N. Sakai
Department of Chemistry
Georgetown University
Washington, DC 20057-1227 (USA)
Fax: (+1) 202-687-6209
E-mail: matiles@gusun.georgetown.edu

[**] This work was supported by NIH (GM56147), the donors of the Petroleum Research Fund (administered by the American Chemical Society), Research Corporation (Research Innovation Award), Suntory Institute for Bioorganic Research (SUNBOR Grant), and Georgetown University. B.G. is a Fulbright Fellow.

  1433-7851/99/3804-0540 $ 17.50+.50/0

specific mutagenesis and X-ray analysis of K^+ channel proteins.[1] However, the conflicting recent model which also considers the interaction of cations with π electrons of the multiple aromatic amino acid residues in the pore region of K^+ channels continues to attract a great deal of attention as well.[2] Computational studies of benzene-cation-benzene complexes in water with fixed and, more convincingly, with flexible benzene – benzene distances have provided persuasive support for the latter model.[4] Subsequent experimental results with cleverly devised synthetic models[5–7] reaffirmed the anticipated[4] limitations of fixed arene – arene distances, and thus provided additional incentive to explore the potential significance of flexible cyclic arene arrays for K^+ selectivity. Here we report the first synthetic, ligand-gated[8] K^+ channel model with flexible arene – arene distances.

The cell-surface receptor model **1** consists of a ligand binding site, a spacer, and a membrane-spanning, rigid, rod-shaped "π slide" (Figure 1).[9] The iminodiacetate (IDA) group was selected as the external ligand binding site because multivalent binding of IDA to polyhistidine (pHis) through Cu^{2+} has been shown to induce aggregation of IDA – lipid conjugates in lipid bilayers.[10] The IDA group was linked through a hydrophilic spacer to one terminus of a septi(*p*-phenylene). This rigid-rod molecule may serve as a consecutive cation binding site or π slide for cations.[11–13]

Binding and organization of rigid-rod fluorophore **1** in lipid bilayers were investigated using spin-labeled lipids as previously reported for other oligo(*p*-phenylene)s.[11, 13] Compared to the emission intensity of **1** at 380 nm in unlabeled EYPC-SUVs, the fluorescence of heptamer **1** (5 μM) was quenched about 35 % by both 5- and 12-DOXYL-PC-labeled vesicles.[14] Almost identical quenching efficiencies with differently located spin labels prove transmembrane orientation of the receptor model, as shown in Figure 1.

In the circular dichroism (CD) spectra, the membrane-bound receptor model **1** exhibits a negative Cotton effect (CE) at 305 nm and a broad positive CE at about 260 nm centered around the red-shifted absorption maximum at 285 nm (Figure 2, curves a and g). The dependence of the CD absorption ($\Delta\varepsilon$) on the oligophenylene concentration implies that the observed induced CD originates from intermolecular exciton coupling within a ligand-free self-assembly **2**.[15] The additional presence of membrane-bound receptor models **3** cannot, however, be excluded.

The addition of increasing concentrations of the multivalent ligand pHis caused a hypsochromic shift of the absorption maximum and a strong increase of the bathochromic CE; changes of the broad positive CE below 275 nm were obscured by contributions of pHis and light scattering from the vesicles (Figure 2). Consistent with ligand-induced formation of transmembrane, well-ordered "H" aggregates (or perhaps even of single, chiral "pinwheel" units),[16] these spectroscopic changes were dependent on the concentration of the receptor as well as the ligand/receptor ratio, and were observed neither with the univalent imidazole ligand nor in the absence of $CuCl_2$.

The ion transport activity of the ligand – receptor complex **4** was assessed using EYPC-SUVs with entrapped pH-sensitive fluorophore 8-hydroxypyrene-1,3,6-trisulfonic acid (HPTS) as

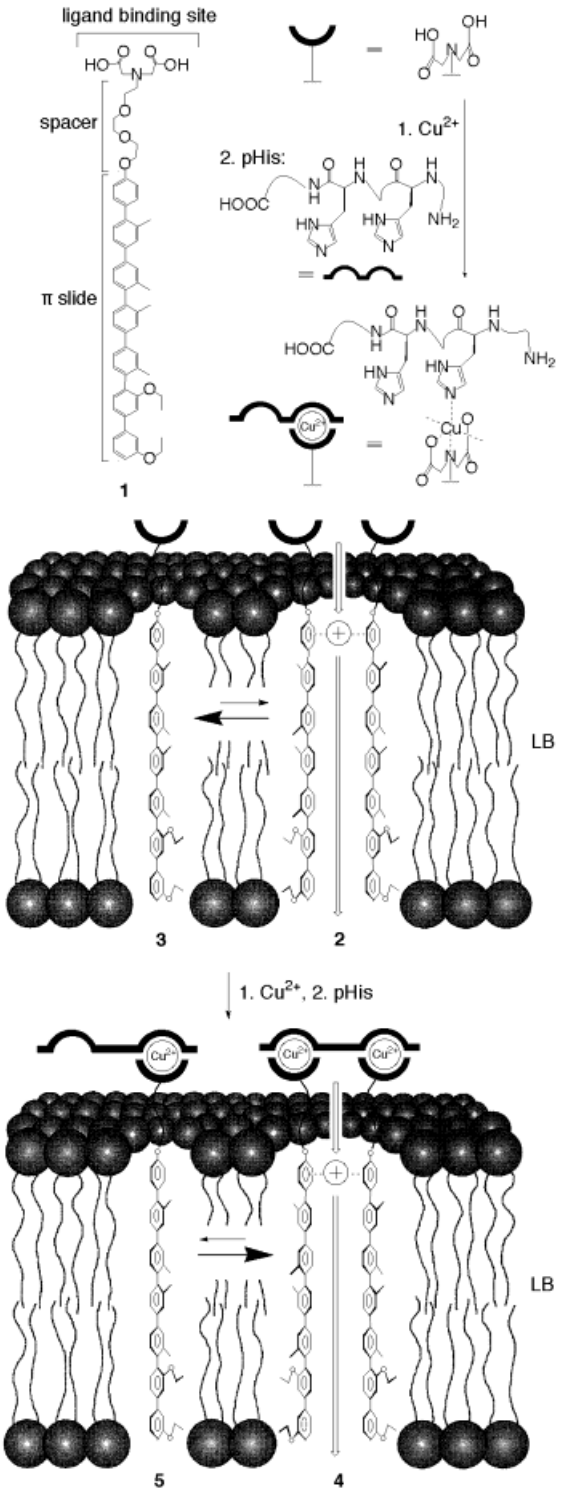

Figure 1. Structure and active suprastructures of receptor model **1**. In all cases, only two oligophenylenes out of an aggregate are shown; ⊕ indicates cations bound to multiple arenes, and → the direction of cation flux during cation/proton exchange (see Figure 3). The structure of pHis (average His/polymer ratio = 104) is simplified. LB = lipid bilayer.

well as high external K^+ and high internal H^+ and Na^+ concentrations (Figure 3 B). Under these conditions, the transport activity of complex **4** (i.e., the rate of intravesicular pH change) was comparable to that of the K^+ channel forming antifungal polyene amphotericin B (AmB; Figure 3 A,

  1433-7851/99/3804-0541 $ 17.50+.50/0

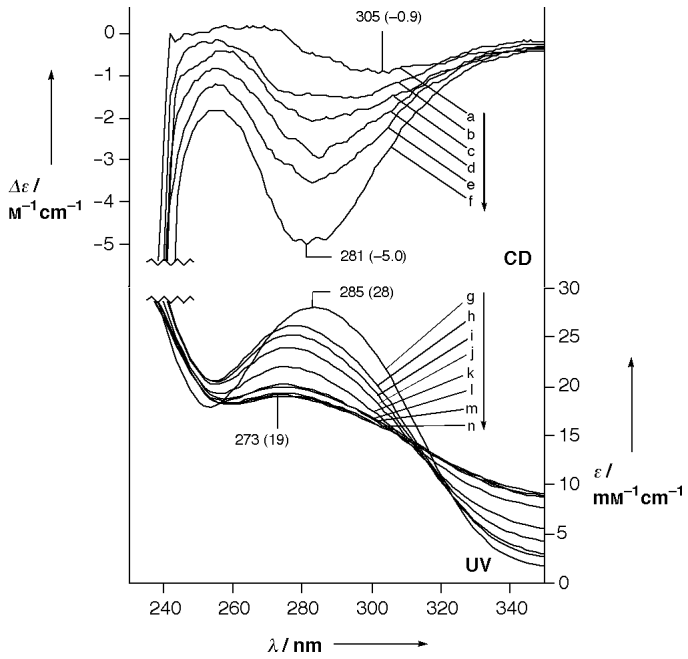

Figure 2. Representative circular dichroism and absorption spectra for receptor model **1** (40 μM) and $CuCl_2$ (60 μM) in the presence of EYPC-SUVs and the following concentrations of pHis [nM]: a) 0, b) 80, c) 100, d) 120, e) 140, f) 160, g) 0, h) 80, i) 100, j) 120, k) 140, l) 160, m) 180, n) 200, 220, and 240.

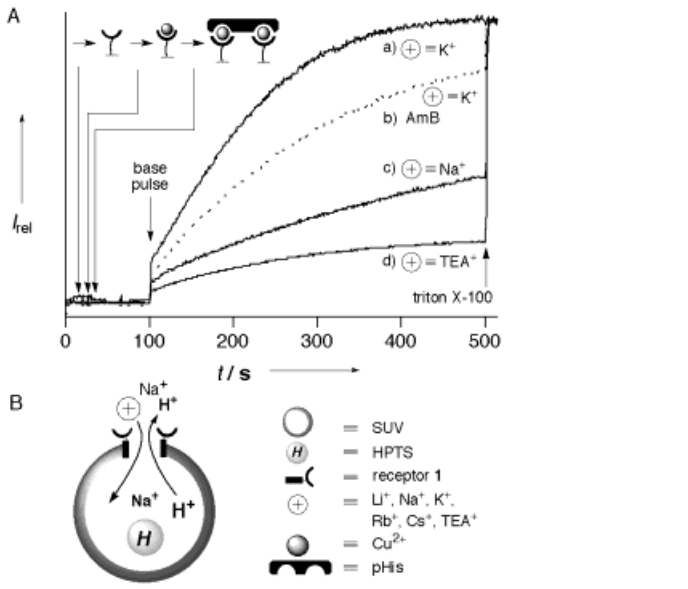

Figure 3. A) Representative cation/proton exchange curves with ligand–receptor complex **4** (2.5 μM **1**, 10 μM $CuCl_2$, ≈0.2 μM pHis) and various extravesicular salts MCl: a) M = K, b) AmB (2.5 μM) with extravesicular K^+ without Cu–pHis, c) M = Na, d) M = TEA. Intravesicular pH was monitored ratiometrically [$I_t = I_a(\lambda_{em} = 510$ nm, $\lambda_{ex} = 460$ nm)/$I_b(\lambda_{em} = 510$ nm, $\lambda_{ex} = 405$ nm)] and normalized [$(I_t - I_0)/(I_\infty - I_0)$]. B) Schematic representation of the transport experiments.

curves a and b).[17] Replacement of the external K^+ with identical concentrations of Rb^+, Cs^+, Li^+, and Na^+ gave up to 3.1-times reduced rates (Figure 3A, curves a and c). This increased transport selectivity for K^+ with respect to Na^+ is among the highest observed so far with synthetic models.[5, 18]

The selectivity topology of transmembrane ion transport mediated by supramolecule **4**, an Eisenman sequence IV with a "lithium anomaly", is similar to that of the permeability ratios of K^+ channel proteins (Figure 4, ■, □, ●).[19] The

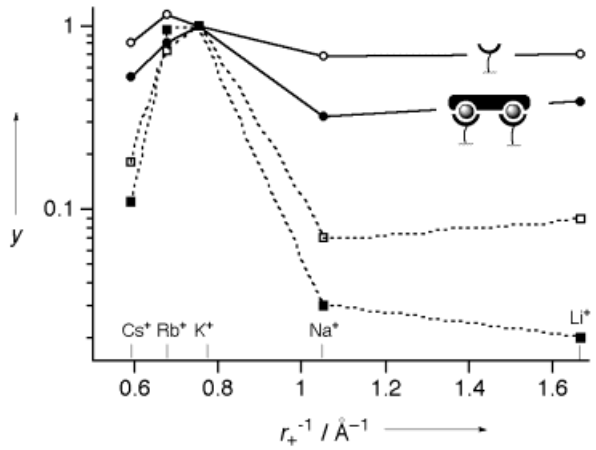

Figure 4. The selectivity topology y of two K^+ channels and model compound **1**. The logarithm of permeability ratios (for K^+ channels),[19] or the logarithm of transport efficiency ratios (for models), is plotted against the reciprocal cation radius; (□) delayed K^+ current, helix neurons; (■) delayed K^+ current, skeletal muscle; (●) membrane-bound ligand–receptor complex **4**; (○) membrane-bound ligand-free receptor **2**.

selectivity for the ligand-free supramolecule **2** is lower than that of **4**, and its topology is an Eisenman sequence III, indicating weaker interactions between ion and binding site (Figure 4, ○). The higher field strength of supramolecule **4** compared to that of ligand-free receptor **2** strongly implies ligand-induced organization of the π slides to form consecutive cyclic cation binding sites, which is in good agreement with the spectroscopic results (Figure 2).

In the presence of external tetraethylammonium cation (TEA^+), transmembrane ion transport mediated by **4** was practically inhibited (Figure 3A, curve d). TEA^+ is a potent K^+ channel blocker that is thought to act by binding to a cyclic arene tetrad in the ion-conducting pore.[1] Thus, TEA^+ blockage of **4** further supports that the observed ion selectivity originates with all likelihood from ligand-assembled, consecutive arene arrays.

In conclusion, we have demonstrated that transmembrane ion transport by ligand-assembled π slides occurs with a selectivity topology comparable to that of K^+ channels, and can be inhibited by a common K^+ channel blocker. These results imply that flexible, "dynamic" arene arrays may indeed contribute to the selectivity of K^+ channels.

Experimental Section

EYPC-SUVs were prepared as previously reported,[11] but with phosphate buffer (10 mM Na_2HPO_4/NaH_2PO_4, pH 6.4, 100 mM NaCl (negative controls: 100 mM LiCl), 0.1 mM HPTS). For a transport experiment, an MCl buffer (1750 μL; 10 mM Na_2HPO_4/NaH_2PO_4, pH 6.4, 100 mM MCl, M = Cs, Rb, K, Na, Li, or TEA) was placed in a thermostated fluorescence cell, and an aliquot (50 μL) of EYPC-SUVs stock solution (10 mM) was added. To the stirred suspension, 250 μM **1** in DMSO/THF (20 μL, positive control: 250 μM AmB, negative control: DMSO/THF), 1 mM $CuCl_2$ (20 μL; for AmB/**2**: MCl buffer), MCl buffer (200 μL) with ca. 2 μM pHis (Sigma, for

  1433-7851/99/3804-0542 $ 17.50+.50/0 *Angew. Chem. Int. Ed.* **1999**, *38*, No. 4

AmB/**2**: MCl buffer), and 0.5 M NaOH (20 μL) were subsequently added. Usually 400 sec after the base pulse, 10% triton X-100 (50 μL) was added to determine complete collapse of the pH gradient (final pH 7.4). Relative transport efficiencies were calculated from the initial rate constants in comparison to that with external K^+ ($k = 1.6 \times 10^{-2} s^{-1}$), and are given in Figure 4. The CD, UV/Vis, and fluorescence quenching experiments were performed as reported before.[11]

Received: May 29, 1998
Revised version: September 25, 1998 [Z11921IE]
German version: *Angew. Chem.* **1999**, *111*, 523 – 526

Keywords: ion channels · ligand effects · membranes · protein mimetics · supramolecular chemistry

[1] D. A. Doyle, J. M. Cabral, R. A. Pfuetzner, A. Kuo, J. M. Gulbis, S. L. Cohen, B. T. Chait, R. MacKinnon, *Science* **1998**, *280*, 69.
[2] D. A. Dougherty, *Science* **1996**, *271*, 163.
[3] C. Miller, *Science* **1991**, *252*, 1092.
[4] R. A. Kumpf, D. A. Dougherty, *Science* **1993**, *261*, 1708.
[5] Y. Tanaka, Y. Kobuke, M. Sokabe, *Angew. Chem.* **1995**, *107*, 717; *Angew. Chem. Int. Ed. Engl.* **1995**, *34*, 693.
[6] P. Schmitt, P. D. Beer, M. G. B. Drew, P. D. Sheen, *Angew. Chem.* **1997**, *109*, 1926; *Angew. Chem. Int. Ed. Engl.* **1997**, *36*, 1840.
[7] N. Kimizuka, T. Wakiyama, A. Yanagi, S. Shinkai, T. Kunitake, *Bull. Chem. Soc. Jpn.* **1996**, *69*, 3681.
[8] T. M. Fyles, B. Zeng, *Chem. Commun.* **1996**, 2295.
[9] The synthesis of **1** is described in: B. Ghebremariam, S. Matile, *Tetrahedron Lett.* **1998**, *39*, 5335.
[10] K. M. Maloney, D. R. Shnek, D. Y. Sasaki, F. H. Arnold, *Chem. Biol.* **1996**, *3*, 185, and references therein.
[11] L. A. Weiss, N. Sakai, B. Ghebremariam, C. Ni, S. Matile, *J. Am. Chem. Soc.* **1997**, *119*, 12142.
[12] N. Sakai, K. C. Brennan, L. A. Weiss, S. Matile, *J. Am. Chem. Soc.* **1997**, *119*, 8726.
[13] C. Ni, S. Matile, *Chem. Commun.* **1998**, 755.
[14] DOXYL = 2,2-disubstituted-4,4-dimethyl-3-oxazolidinyloxy, free radical, EYPC-SUVs: small unilamellar vesicles composed of egg yolk phosphatidylcholine; 5-DOXYL-PC: 1-palmitoyl-2-stearoyl(5-DOXYL)-*sn*-glycero-3-phosphocholine; 12-DOXYL-PC: 1-palmitoyl-2-stearoyl(12-DOXYL)-*sn*-glycero-3-phosphocholine.
[15] K. Nakanishi, N. Berova in *Circular dichroism—principles and applications* (Eds.: K. Nakanishi, N. Berova, R. W. Woody), VCH, New York, **1994**, p. 361.
[16] a) X. Song, J. Perlstein, D. G. Whitten, *J. Am. Chem. Soc.* **1997**, *119*, 9144; b) X. Song, C. Geiger, U. Leinhos, J. Perlstein, D. G. Whitten, *J. Am. Chem. Soc.* **1994**, *116*, 10340; c) D. G. Whitten, *Acc. Chem. Res.* **1993**, *26*, 502.
[17] a) S. C. Hartsel, S. K. Benz, R. P. Peterson, B. S. Whyte, *Biochemistry* **1991**, *30*, 77; b) J. Bolard, P. Legrand, F. Heitz, B. Cybulska, *Biochemistry* **1991**, *30*, 5707.
[18] G. W. Gokel, O. Murillo, *Acc. Chem. Res.* **1996**, *29*, 425.
[19] G. Eisenman, R. Horn, *J. Membrane Biol.* **1983**, *76*, 197.

Easy Access to Soluble Polyanions—Stabilization of the One-Dimensional Chain $^1_\infty[K_4Sn_9]$ by [18]Crown-6 in $[K_4Sn_9([18]crown\text{-}6)_3] \cdot ethylenediamine$**

Thomas F. Fässler* and Rudolf Hoffmann

Dedicated to Professor Ernst Otto Fischer on the occasion of his 80th birthday

The reduction of metal salts provides an important way for the synthesis of element nanoparticles. Though routes for the generation of large transition metal clusters are well elaborated,[1] comparably little is known about analogous accesses to main group element clusters.[2] A general problem of the synthesis of nanoparticles is the broad distribution of particle size.[3] In contrast, a directed synthesis of small, charged main group element clusters of uniform size exists, and recently the chemistry of homoatomic clusters of Group 14 elements received new impulses through the synthesis and structure determination of the phases $Rb_{12}Si_{17}$,[4] A_4Ge_9 (A = K, Cs),[5, 6] $K_{12}Ge_{17}$,[5] and K_4Pb_9.[7] The crystalline compounds, which are synthesized from the elements at several hundred degrees, are Zintl phases with discrete nine-atom E_9^{4-} clusters. In the case of the 12:17 phases additional tetrahedral E_4^{4-} units are present. The crystal structure of the corresponding phase A_4Sn_9 or $A_{12}Sn_{17}$ (A = alkali metal) could not be elucidated due to poor crystal quality.[6] Though nine-atom clusters were observed in solution over 100 years ago[8] and the first structural characterization was carried out already in 1976,[9] only small amounts of well-defined products could be isolated from solution. In the course of our studies of soluble, homoatomic Zintl ions,[10] we report here a novel, very simple and efficient access to homoatomic polyanions from the elements at low temperatures.

We found that the alkali metals K, Rb, and Cs are soluble in the crown ether [18]crown-6, which is liquid at 40 °C.[11] The deep blue color of the melt indicates the formation of an alkalide or electride. The blue color vanishes after addition of an element of Group 14 to 16, indicating a reaction. To obtain crystalline products small amounts of solvent are added to the mixture. So far we were able to apply this procedure to the elements C (as C_{60}), Sn, Pb, As, Sb, Bi, and Te. Single-crystal structure analyses reveal the presence of the anions C_{60}^{3-},[12a] Sn_9^{4-}, Pb_9^{4-}, As_7^{3-}, Sb_7^{3-}, and Te_4^{2-}.[12b] For As, Sb,[13] and Te,[14] the formation of larger homoatomic polyanions in solution from the elements and their isolation in crystalline form was already known. However, in the case of Sn and Pb crystalline products were only obtained by extraction of binary or ternary phases.[15] With the exception of $[Na_4(en)_7]Sn_9$, which was characterized by Kummer and Strähle and which contains disordered en molecules (en = ethylenediamine),[16] the struc-

[*] Priv.-Doz. Dr. T. F. Fässler, R. Hoffmann
Laboratorium für Anorganische Chemie
der Eidgenössischen Technischen Hochschule
Universitätstrasse 6, CH-8092 Zürich (Switzerland)
Fax: (+41) 1-632-1149
E-mail: faessler@inorg.chem.ethz.ch

[**] This work has been supported by the ETH Zürich and the Swiss National Science Foundation.